Research Article | Vol. 25, No. 3 | 6 Feb 2017 | OPTICS EXPRESS 2239

Optics EXPRESS

# Experimental study on depolarized GAWBS spectrum for optomechanical sensing of liquids outside standard fibers

**NEISEI HAYASHI,[1,*] YOSUKE MIZUNO,[2] KENTARO NAKAMURA,[2] SZE YUN SET,[1] AND SHINJI YAMASHITA[1]**

[1]*Research Center for Advanced Science and Technology, The University of Tokyo, 4-6-1, Komaba, Meguro-ku, Tokyo 153-8904, Japan*
[2]*Institute of Innovative Research, Tokyo Institute of Technology, 4259, Nagatsuta-cho, Midori-ku, Yokohama 226-8503, Japan*
**hayashi@cntp.t.u-tokyo.ac.jp*

**Abstract:** We report an experimental study on the spectral dependence of depolarized guided acoustic-wave Brillouin scattering (GAWBS) in a silica single-mode fiber (SMF) on acoustic impedance of external materials. The GAWBS spectrum was measured when the acoustic impedance was changed from 1.51 to 2.00 kg/s·mm$^2$. With increasing acoustic impedance, the linewidth increased; the dependence was almost linear with an acoustic impedance dependence coefficient of 0.16 MHz/kg/s·mm$^2$. Meanwhile, with increasing acoustic impedance, the central frequency linearly decreased with an acoustic impedance dependence coefficient of –0.07 MHz/kg/s·mm$^2$. These characteristics are potentially applicable to acoustic impedance sensing.



**OCIS codes:** (060.2370) Fiber optics sensors; (120.0280) Remote sensing and sensors; (280.4788) Optical sensing and sensors.

## References and links

1. R. M. Shelby, M. D. Levenson, and P. W. Bayer, "Guided acoustic-wave Brillouin scattering," Phys. Rev. B Condens. Matter **31**(8), 5244–5252 (1985).
2. A. J. Poustie, "Bandwidth and mode intensities of guided acoustic-wave Brillouin scattering in optical fibers," J. Opt. Soc. Am. B **10**(4), 691–696 (1993).
3. Y. Antman, A. Clain, Y. London, and A. Zadok, "Optomechanical sensing of liquids outside standard fibers using forward stimulated Brillouin scattering," Optica **3**(5), 510–516 (2016).
4. T. Horiguchi and M. Tateda, "BOTDA–nondestructive measurement of single-mode optical fiber attenuation characteristics using Brillouin interaction: Theory," J. Lightwave Technol. **7**(8), 1170–1176 (1989).
5. J. Urricelqui, M. Sagues, and A. Loayssa, "Phasorial differential pulse-width pair technique for long-range Brillouin optical time-domain analysis sensors," Opt. Express **22**(14), 17403–17408 (2014).
6. Y. Dong, L. Teng, P. Tong, T. Jiang, H. Zhang, T. Zhu, L. Chen, X. Bao, and Z. Lu, "High-sensitivity distributed transverse load sensor with an elliptical-core fiber based on Brillouin dynamic gratings," Opt. Lett. **40**(21), 5003–5006 (2015).
7. Y. Dong, D. Ba, T. Jiang, D. Zhou, H. Zhang, C. Zhu, Z. Lu, H. Li, L. Chen, and X. Bao, "High-spatial-resolution fast BOTDA for dynamic strain measurement based on differential double-pulse and second-order sideband of modulation," IEEE Photonics J. **5**(3), 2600407 (2013).
8. T. Kurashima, T. Horiguchi, H. Izumita, S. Furukawa, and Y. Koyamada, "Brillouin optical-fiber time domain reflectometry," IEICE Trans. Commun. **E76-B**(4), 382–390 (2014).
9. L. E. Y. Herrera, G. C. Amaral, and J. P. von der Weid, "Investigation of bend loss in single mode fibers with ultra-high-resolution photon-counting optical time domain reflectometer," Appl. Opt. **55**(5), 1177–1182 (2016).
10. K. Hotate and T. Hasegawa, "Measurement of Brillouin gain spectrum distribution along an optical fiber using a correlation-based technique—Proposal, experiment and simulation—," IEICE Trans. Electron. **E83-C**(3), 405–412 (2000).
11. R. K. Yamashita, W. Zou, Z. He, and K. Hotate, "Measurement range elongation based on temporal gating in Brillouin optical correlation domain distributed simultaneous sensing of strain and temperature," IEEE Photonics Technol. Lett. **24**(12), 1006–1008 (2012).
12. Y. Mizuno, W. Zou, Z. He, and K. Hotate, "Proposal of Brillouin optical correlation-domain reflectometry (BOCDR)," Opt. Express **16**(16), 12148–12153 (2008).
13. N. Hayashi, Y. Mizuno, and K. Nakamura, "Distributed Brillouin sensing with centimeter-order spatial resolution in polymer optical fibers," J. Lightwave Technol. **32**(21), 3399–3401 (2014).

#280890 https://doi.org/10.1364/OE.25.002239
Journal © 2017 Received 9 Dec 2016; revised 22 Jan 2017; accepted 24 Jan 2017; published 27 Jan 2017

Optics EXPRESS

14. Y. Mizuno, N. Hayashi, H. Fukuda, K. Y. Song, and K. Nakamura, "Ultrahigh-speed distributed Brillouin reflectometry," Light Sci. Appl. **5**(12), e16184 (2016).
15. Schlumberger Limited, *Log Interpretation Principles/ Applications* (Schlumberger Educational Services, Texas, 1991).
16. M. L. Palmeri, M. H. Wang, N. C. Rouze, M. F. Abdelmalek, C. D. Guy, B. Moser, A. M. Diehl, and K. R. Nightingale, "Noninvasive evaluation of hepatic fibrosis using acoustic radiation force-based shear stiffness in patients with nonalcoholic fatty liver disease," J. Hepatol. **55**(3), 666–672 (2011).
17. Y. Kato, Y. Wada, Y. Mizuno, and K. Nakamura, "Measurement of elastic wave propagation velocity near tissue surface through optical coherence tomography and laser Doppler velocimetry," Jpn. J. Appl. Phys. **53**(7S), 07KF05 (2014).
18. Y. Tanaka, H. Yoshida, and T. Kurokawa, "Guided-acoustic-wave Brillouin scattering observed backward by stimulated Brillouin scattering," Meas. Sci. Technol. **15**(8), 1458–1461 (2004).
19. N. Hayashi, H. Lee, Y. Mizuno, and K. Nakamura, "Observation of backward guided-acoustic-wave Brillouin scattering in optical fibers using pump-probe technique," IEEE Photonics J. **8**(3), 7100707 (2016).
20. Y. Tanaka and K. Ogusu, "Tensile-strain coefficient of resonance frequency of depolarized guided acoustic-wave Brillouin scattering," IEEE Photonics Technol. Lett. **11**(7), 865–867 (1999).
21. Y. Tanaka and K. Ogusu, "Temperature coefficient of sideband frequencies produced by depolarized guided acoustic-wave Brillouin scattering," IEEE Photonics Technol. Lett. **10**(12), 1769–1771 (1998).
22. M. Ohashi, S. Naotaka, and S. Kazuyki, "Fibre diameter estimation based on guided acoustic wave Brillouin scattering," Electron. Lett. **28**(10), 900–902 (1992).
23. B. I. Greene and P. N. Saeta, "Low-frequency line shapes in guided acoustic-wave Brillouin scattering," Appl. Phys. Lett. **65**(18), 2269–2271 (1994).
24. J. Saneyoshi, Y. Kikuchi, and O. Nomoto, *Cho-onpa Gijutsu Binran (Handbook of Ultrasonic Technology)* (Nikkan Kogyo, 1978).
25. J. Wang, Y. Zhu, R. Zhang, and D. J. Gauthier, "FSBS resonances observed in a standard highly nonlinear fiber," Opt. Express **19**(6), 5339–5349 (2011).

## 1. Introduction

Guided acoustic-wave Brillouin scattering (GAWBS), one of the nonlinear phenomena in an optical fiber, occurs by the interaction between incident light and acoustic waves propagating in the cross-sectional area of the fiber [1]. This scattering is known to be forward scattering that accompanies multiple spectral peaks caused by acoustic resonance. Its spectrum depends on several fiber structural parameters, such as a fiber outer diameter, a core diameter, and a refractive index profile [2]. GAWBS can be categorized into two types: one is polarized GAWBS caused by the radial-mode ($R_{0,m}$) acoustic waves [1], and the other is depolarized GAWBS caused by the torsional-radial-mode ($TR_{2,m}$) acoustic waves [1], where $m$ denotes the order of the acoustic resonance. The $R_{0,m}$ mode perturbs the refractive index of the fiber cross section, while the $TR_{2,m}$ mode perturbs not only the refractive index but also the birefringence [1].

Very recently, the idea of acoustic impedance sensing based on polarized GAWBS has also been proposed [3]. The basic principle of this acoustic impedance sensing lies in the amplitude dependence of the $R_{0,m}$-mode acoustic waves on the acoustic reflection between the cladding and overcladding/outside material. However, this sensing technique suffers from a drawback that it is difficult to apply existing distributed sensing techniques [4–14] because of the ring-shaped configuration of the fiber under test (FUT). Distributed acoustic impedance sensing based on GAWBS will open up new applications in future, such as underground oil layer detection without employing external vibrations [15] and cancer detection in the human body exploiting the stiffness difference between normal cells and diseased cells [16,17].

In order to overcome these drawbacks, here we focus on the use of depolarized GAWBS, which has been experimentally shown to efficiently couple with backscattered stimulated Brillouin scattering, providing a potential for distributed GAWBS sensing [18,19]. To date, some sensing characteristics of depolarized GAWBS have been investigated, including the central frequency dependence on strain, ambient temperature, and fiber outer diameter [20–22]. In [2], the linewidth is shown to change by external acoustic impedance. However, a detailed experimental study on the acoustic impedance dependence of the central frequency and the linewidth of the depolarized GAWBS has not been performed yet to the best of our knowledge.

Optics EXPRESS

In this paper, we measure the external acoustic impedance dependence of depolarized GAWBS in an unjacketed silica single-mode fiber (SMF) immersed into sucrose solution with 0–65% concentration (corresponding to the acoustic impedance ranging from 1.51 to 2.00 kg/s·mm$^2$). The spectral linewidth increases nonlinearly with increasing acoustic impedance; the dependence in the range is almost linear with a coefficient of 0.16 MHz/kg/s·mm$^2$. In the meantime, as the acoustic impedance increases, the central frequency decreases, which probably originates from the increase in the effective outer diameter of the fiber. The dependence is almost linear with a coefficient of −0.07 MHz/kg/s·mm$^2$, the sign of which is opposite to the strain and temperature coefficients. These features could be exploited to acoustic impedance sensing. As both the linewidth and the central frequency of the depolarized GAWBS spectrum are independently changed with acoustic impedance, by using these two parameters simultaneously, discriminative sensing of acoustic impedance and strain (or temperature) might be feasible.

## 2. Principle

There exist various kinds of acoustic waves in optical fibers caused by thermal fluctuations [1,2]. Among these acoustic waves, that of the torsional-radial acoustic mode ($TR_{2,m}$, where $m$ is the acoustic resonance mode), which literally induces displacements not only in the radial direction but also in the torsional direction, perturbs the refractive index and birefringence in the fiber [1,2]. The optical scattering by this acoustic mode is called depolarized GAWBS, which poses multiple spectral peaks of up to several gigahertz. The central frequency (GAWBS-induced frequency shift) of the $m$-th acoustic mode ($\nu_{GB,m}$) is given by [1]

$$\nu_{GB,m} = \frac{v_s y_m}{\pi d}, \tag{1}$$

where $d$ is the fiber outer diameter, $v$ is the velocity of the shear acoustic waves $v_s$ (for depolarized GAWBS; this should be interpreted as the velocity of longitudinal acoustic waves $v_L$ for polarized GAWBS). The symbol $y_m$ is the value derived from the following equation [1]:

$$\begin{vmatrix} (3-\frac{y_m^2}{2})J_2(\alpha y_m) & (6-\frac{y_m^2}{2})J_2(y_m)-3y_m J_3(y_m) \\ J_2(\alpha y_m)-\alpha y_m J_3(\alpha y_m) & (2-\frac{y_m^2}{2})J_2(y_m)-y_m J_3(y_m) \end{vmatrix} = 0, \tag{2}$$

where $\alpha$ is $v_s/v_L$ ( = 0.624 [3]), and $J_2$ and $J_3$ are the second- and third-order Bessel functions. The central frequency is known to depend on strain and temperature with dependence coefficients ($m$ = 5) of 1.9 MHz/% and 11 kHz/K, respectively [20,21]. Meanwhile, the spectral linewidth $\Delta_{GB}$ can be estimated by [23]:

$$\Delta_{GB} = \frac{v_s \beta}{\pi}, \tag{3}$$

where $\beta$ is the acoustic loss, which includes the propagation loss in the optical fiber and the reflection loss at the boundary between the cladding and the external material [2,23].

## 3. Experimental setup and method

As an FUT, we employed an unjacketed 17-m-long silica SMF with a core diameter of 10.0 μm, a cladding diameter of 125.8 μm, a core refractive index of ~1.46, and a propagation loss of ~0.2 dB/km at 1.55 μm. The FUT was immersed into sucrose solution in a water bath, the concentration of which was controlled in the range from 0 to 45% to obtain arbitrary acoustic

Optics EXPRESS

impedance (see Table 1; cited from [24]). The temperature of the sucrose solution was kept to the 26.5 °C (which equals room temperature).

A schematic setup for observing the depolarized GAWBS spectrum is depicted in Fig. 1, which is basically the same as that previously reported [20,21]. All the optical paths including the FUT were silica SMFs. The output from a distributed-feedback laser diode at 1.55 μm (linewidth: 15 kHz, power: 15 dBm (maximal output)) was injected into the FUT as pump light. Subsequently, the optical beat signal of the GAWBS forward-scattered light and the pump light was guided to a polarizer (PL) and then to a photo detector (PD) for optical-to-electrical conversion. The signal was finally monitored as GAWBS spectrum using an electrical spectrum analyzer (ESA) with a 1-kHz frequency resolution and a 54-kHz video bandwidth. Averaging was performed 1000 times. The peak power of the depolarized GAWBS spectrum was maximized using polarization controllers (PCs), which indicates that the light beam can be regarded as a depolarized beam [20,21].

In this measurement, we selectively observed the spectral peak corresponding to the $TR_{2,5}$ mode [20], which exhibited the highest signal-to-noise ratio of all the other peaks [1]. We performed noise-floor compensation in the following procedure: (i) the raw data of the GAWBS spectrum was obtained using the ESA, (ii) the noise floor (the spectrum when the FUT was removed from the experimental setup) was separately obtained, (iii) the noise floor was subtracted from the raw data, and (iv) the obtained spectrum was fitted by a Lorentzian curve [25]. Figure 2(a) shows the raw GAWBS spectrum of the$TR_{2,5}$ mode. A clear peak was observed at 108.48 MHz (corresponding to $v_s$ = 3765 m/s; theoretical value: 107.7 MHz), but the spectral shape was slightly distorted. The measurement error of the center frequency was less than ± 0.006 MHz, which was calculated as a standard deviation of eight measured data (obtained every 5 min). Figure 2(b) then shows the obtained noise floor, which included a small peak at 107.87 MHz. Finally, the subtracted spectrum is shown in Fig. 2(c). The spectral distortion was mitigated; the Lorentzian fit of this spectrum was used for GAWBS characterization. The linewidth $\Delta_{GB}$ was measured to be 0.211 MHz, and the acoustic loss $\beta$ was estimated to be 178 $m^{-1}$. The measurement error of the linewidth (calculated in the same method as that of the center frequency) was less than ± 0.001 MHz.

**Table 1. Acoustic impedance of sucrose solution.**

| Concentration [%] | 0 | 10 | 20 | 30 | 40 | 45 |
|---|---|---|---|---|---|---|
| Acoustic impedance [kg/s·mm$^2$] [a] | 1.51 | 1.58 | 1.68 | 1.79 | 1.92 | 2.00 |

[a]Ref. 24

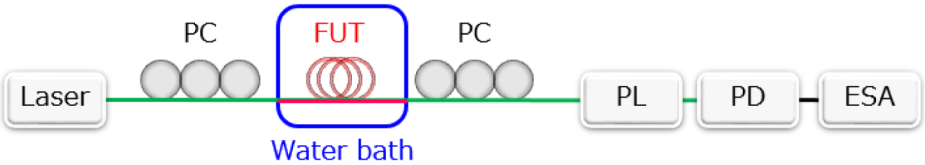


Fig. 1. Schematic setup for observing depolarized GAWBS. ESA, electrical spectrum analyzer; PC, polarization controller; PD, photo detector; PL, polarizer.

Optics EXPRESS

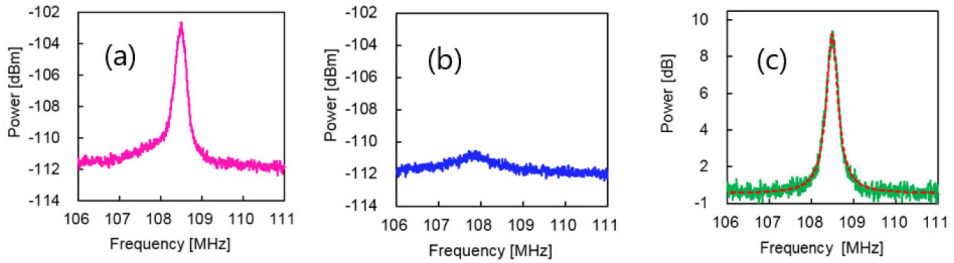


Fig. 2. Depolarized GAWBS spectra corresponding to the $TR_{2,5}$ mode. (a) Raw data, (b) noise floor, and (c) compensated plot. The dotted line in (c) indicates its Lorentzian fit.

## 4. Experimental results

The normalized depolarized GAWBS spectral dependence on external acoustic impedance is shown in Fig. 3(a). The spectrum changed with the increase of acoustic impedance. The spectral peak power did not show a clear dependence on the acoustic dependence. From this measurement, the dependences of the linewidth and the central frequency on external acoustic impedance can be plotted. Figure 3(b) shows the linewidth dependence on acoustic impedance; here, the linewidth was defined as the full width at half maximum of the 3-dB spectral bandwidth. The linewidth increased as the acoustic impedance increased, and the dependence in the acoustic impedance range below 2.0 kg/s·mm$^2$ was almost linear with a coefficient of 0.16 MHz/kg/s·mm$^2$. Note that this is a relative measurement, but a quantitative absolute measurement might be feasible by theoretically analyzing the $TR_{2,5}$-mode acoustic-wave model with boundary conditions, referring to the method proposed in [3]. Figure 3(c) shows the central frequency dependence on acoustic impedance. With increasing acoustic impedance, the central frequency linearly decreased with a coefficient of –0.07 MHz/kg/s·mm$^2$. The sign of this value was opposite to the strain and temperature coefficients [3,20,21]. Considering Eq. (1), this may be elucidated by the solutions of the elastic wave equations with the boundary conditions of a finite (non-vacuum) surrounding medium; further study is required on this point. As the linewidth and the central frequency of the depolarized GAWBS spectrum were linearly changed with external acoustic impedance, they can be potentially used to perform acoustic impedance sensing. Besides, combined use of the linewidth and the central frequency may enable discriminative sensing of acoustic impedance and another parameter, such as strain and temperature, as stated in [3]. Note that the repeatability of these results was confirmed to be high by performing the same measurements using other FUTs.

Optics EXPRESS

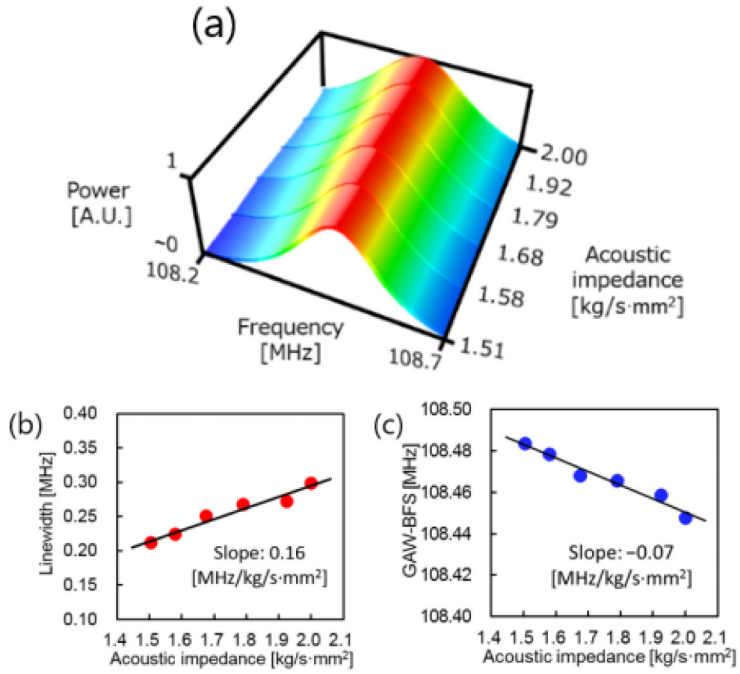


Fig. 3. Measured acoustic impedance dependences of (a) depolarized GAWBS spectrum, (b) its linewidth, and (c) its central frequency.

## 5. Conclusions

The acoustic impedance dependence of the depolarized GAWBS spectrum in an unjacketed silica SMF was experimentally studied. The FUT was immersed into sucrose solution with the acoustic impedance ranging from 1.51 to 2.00 kg/s·mm$^2$. As the acoustic impedance was increased, the spectral linewidth linearly increased with a coefficient of 0.16 MHz/kg/s·mm$^2$. In contrast, as the acoustic impedance increased, the central frequency linearly decreased with a coefficient of –0.07 MHz/kg/s·mm$^2$, the sign of which was opposite to those of the temperature and strain coefficients; this trend may be caused by the increase in the effective outer diameter of the SMF. These results indicate that both the linewidth and the central frequency of the depolarized GAWBS spectrum can be exploited to perform acoustic impedance sensing. We also showed a potential for discriminative sensing of acoustic impedance and another physical parameter. We believe that these findings will be of great use in developing depolarized-GAWBS-based distributed acoustic impedance sensors in the near future for underground oil layer detection and cancer detection in the human body.

## Funding

JSPS KAKENHI (JP15H4012, 25709032, 26630180, 25007652); Japan Gas Association; ESPEC Foundation for Global Environment Research and Technology; Association for Disaster Prevention Research.